Chromosome 1 Aneuploidy Regulates White–Opaque Switching in *Candida albicans*

A Thesis

Submitted in Partial Fulfillment of the Requirements for the

Degree of Master of Science

by

Kritika Maharjan

Advisor: Richard Bennett, PhD

Department of Biology and Medicine

Brown University

2026

This thesis by Kritika Maharjan is accepted in its present form by the Graduate Program in Biotechnology as satisfying the thesis requirements for the degree of Master of Science

Date 4/20/26 Signature: _____

Dr. Richard Bennett, Advisor

Date 4/20/26 Signature: _____

Dr. Christina Cuomo, Reader

Date 4/20/2026 Signature: _____

Dr. Diana Horrigan, Reader

Approved by the Graduate Council

Date _____ Signature: _____

Table of Contents

Abstract
1. Introduction
2. Background
  2.1 *Candida albicans* as a Fungal Pathogen
  2.2 White–Opaque Phenotypic Switching
  2.3 *WOR1* and the Switching Regulatory Network
  2.4 Chromosome 1 and Aneuploidy in *C. albicans*
  2.5 CRISPR/Cas9 as a Tool in *C. albicans*
3. Materials and Methods
  3.1 Strains and Culture Conditions
  3.2 CRISPR/Cas9-Mediated Fluorescent Marker Integration
  3.3 Segmental Chromosomal Deletions
  3.4 Gene Knockouts: *TUP1* and *WOR1*
  3.5 White–Opaque Switching Assays
  3.6 Fluorescence Microscopy and Image Analysis
  3.7 Whole-Genome Sequencing and Coverage Analysis
  3.8 Telomere-Mediated Chromosomal Truncation
4. Results
  4.1 Chr1 Trisomy Suppresses Switching; Chr1 Loss Drives Hyper switching
  4.2 Fluorescent Markers Enable Live Tracking of Chr1 Copy Number
  4.3 *TUP1* Heterozygous Knockout Produces Variable Switching Outcomes
  4.4 Segmental Deletions Identify Regions B and D as Switching Modulators
  4.5 Combined B+D Deletion Induces Hyper switching Without Full Chr1 Loss
  4.6 Telomere-Mediated Truncation: Construct Development
5. Discussion
6. Conclusions
7. References

Abstract

Candida albicans is a major human fungal pathogen capable of undergoing white-opaque phenotypic switching, a stable, heritable, and reversible transition between two distinct cell states that influences mating, host colonization, and immune evasion. The master transcriptional activator of the opaque program, WOR1, resides on Chromosome 1 (Chr1), yet strains carrying three copies of Chr1 (trisomy) show severely reduced switching frequencies, while loss of the extra Chr1 copy drives hyperswitching. This observation suggests that dosage-sensitive repressors encoded on Chr1 outweigh the additional WOR1 copy in the trisomic state, resulting in net suppression of switching.

To identify the chromosomal regions responsible for this suppression, fluorescent reporter strains carrying mNeonGreen and mScarlet markers on distinct Chr1 homologs were engineered to enable live tracking of Chr1 copy number. CRISPR/Cas9-mediated segmental deletions of four Chr1 regions (A, B, C, and D) revealed that regions B and D harbor the dominant switching suppressors. Single deletions of either region produced moderate increases in switching frequency, while their combined deletion in strain BD19 induced hyperswitching approaching that observed upon full Chr1 loss, without requiring deletion of regions A or C. Heterozygous knockout of TUP1, a candidate repressor in region D, produced variable switching outcomes attributable to spontaneous Chr1 arm loss rather than TUP1 dosage alone, consistent with a distributed suppression model. Telomere-mediated chromosomal truncation is under development to dissect the minimal suppressive sub-intervals within regions B and D at higher resolution. Together, these findings demonstrate that Chr1 encodes a distributed network of dosage-sensitive repressors, concentrated in regions B and D, that collectively set the transcriptional threshold for white-opaque switching in C. albicans.

1. Introduction

Candida albicans is one of the most clinically significant fungal pathogens of humans. A commensal organism of the gastrointestinal and urogenital tracts in healthy individuals, it transitions to a pathogenic state in immunocompromised hosts, causing infections ranging from superficial mucosal disease to life-threatening invasive candidiasis. Invasive candidiasis affects an estimated 400,000 people globally each year, with mortality rates of 30–40% even with antifungal treatment (Kullberg & Arendrup, 2015; Pappas et al., 2018). The high mortality reflects both the virulence of this pathogen and the limited arsenal of antifungal agents, understanding its biology is therefore important.

A defining feature of *C. albicans* biology is its ability to undergo white–opaque phenotypic switching, a stable, heritable, and reversible transition between two distinct cell states first described by the Soll group (Slutsky et al., 1987). White cells are round, form smooth white colonies, and represent the predominant form during systemic infection. Opaque cells are elongated, form flat gray colonies, and are optimized for mating and colonization of skin epithelia. The two cell types differ in the expression of approximately 1,100 genes and in their interactions with the host immune system (Tsong et al., 2003; Lohse & Johnson, 2009). Because opaque cells can evade certain immune surveillance mechanisms, the ability to switch between states is considered a key component of the pathogen's virulence toolkit.

The molecular switch between white and opaque states is controlled by a transcriptional network centered on *WOR1* (White Opaque Regulator 1), a transcription factor that acts as the master activator of the opaque program (Huang et al., 2006; Zordan et al., 2007). *WOR1* operates through a positive auto-regulatory feedback loop, in which it activates its own transcription, thereby making opaque cell identity self-sustaining once established. Critically, *WOR1* resides on Chromosome 1 (Chr1), and its dosage, determined in part by the copy number of Chr1, is a key determinant of switching frequency.

Recent observations in the WO-1 laboratory strain revealed a clear link between Chr1 aneuploidy and switching behavior. Strains carrying three copies of Chr1 (trisomy) showed severely reduced or absent switching, while rare spontaneous switchers arising in these populations had invariably lost the extra Chr1 copy. This suggested that the extra copy of Chr1 actively suppresses switching, possibly through increased dosage of repressor genes on the chromosome. Conversely, when the extra copy is lost, the repressive threshold is crossed and hyper switching occurs.

This thesis addresses the central question: *which regions of Chromosome 1 are responsible for suppressing white–opaque switching, and which genes within those regions are the key dosage-sensitive regulators?* To answer this, we engineered fluorescent reporter strains to track Chr1 copy number in living cells, performed CRISPR/Cas9-mediated segmental deletions of four Chr1 regions, carried out single-copy knockouts of key regulatory genes, and developed a telomere-mediated truncation strategy for high-resolution dissection of the most functionally relevant region. The results demonstrate that Chr1 regions B and D, acting in concert, harbor the dominant switching suppressors on Chr1, and that their combined loss is sufficient to induce hyper switching without full chromosomal aneuploidy.

2. Background

2.1 *Candida albicans* as a Fungal Pathogen

Candida albicans occupies a dual role in human biology. In immunocompetent individuals, it lives as a harmless commensal organism colonizing the oral cavity, gastrointestinal tract, and urogenital mucosa. However, in the setting of immunosuppression, whether from HIV/AIDS, hematological malignancy, transplantation, or intensive care interventions, *C. albicans* can breach mucosal barriers and invade the bloodstream, causing candidemia and disseminated candidiasis, which carry mortality rates of 30–40% in affected patient populations (Kullberg & Arendrup, 2015).

C. albicans is a diploid organism and a member of the CTG clade of fungi, which uniquely decode the CUG codon as serine rather than leucine. It lacks a conventional sexual cycle under most conditions; however, the white–opaque switching system enables mating under specific environmental conditions (Miller & Johnson, 2002). Its genome (~14.3 Mb across 8 chromosomes) shows high genomic plasticity, with frequent copy number changes and chromosomal rearrangements that contribute to drug resistance (Selmecki et al., 2010).

Key virulence traits include the ability to undergo morphogenetic transitions between yeast, pseudohyphal, and hyphal forms; the secretion of hydrolytic enzymes including proteases and phospholipases; the formation of drug-resistant biofilms; and phenotypic switching. Together these properties allow *C. albicans* to adapt to diverse host niches and to evade both innate and adaptive immune responses (Jacobsen et al., 2012).

2.2 White–Opaque Phenotypic Switching

White–opaque switching was first described by Slutsky et al. (1987) as a spontaneous, heritable, and reversible transition occurring at a frequency of approximately 10^{-3} to 10^{-4} per cell per generation under

standard laboratory conditions. The two cell types differ not only in colony morphology, white colonies appear smooth and convex while opaque colonies are flat and gray, but also at the cellular level. White cells are round and approximately 3–5 μm in diameter, whereas opaque cells are elongated and bean-shaped, roughly 7–10 μm, with a characteristic pimpled cell surface ultrastructure visible by scanning electron microscopy (Anderson et al., 1989).

The two states differ in the expression of approximately 1,100 genes, representing nearly 20% of the *C. albicans genome* (Tsong et al., 2003). Key differences include opaque cells mate more efficiently, express distinct cell wall proteins, and are less susceptible to killing by neutrophils and macrophages (Lohse & Johnson, 2009; Huang et al., 2010). These properties make the switch highly relevant to pathogenesis, particularly in the context of skin and mucosal infections where opaque cells are believed to be the dominant colonizing form.

Importantly, switching frequency is modulated by environmental signals including temperature (lower temperatures favor opaque), carbon source, and the mating-type locus configuration (only *MTL*a/α heterozygous strains can switch) (Miller & Johnson, 2002). This environmental responsiveness suggests that white–opaque switching serves as an adaptation mechanism that allows *C. albicans* to dynamically tailor its phenotype to host microenvironments.

2.3 *WOR1* and the Switching Regulatory Network

WOR1 (White Opaque Regulator 1) encodes a transcription factor that functions as the master regulator of white–opaque switching in *C. albicans*. White cells express *WOR1* at low levels whereas opaque cells express it at high levels through a self-reinforcing positive feedback loop (Huang et al., 2006; Zordan et al., 2007). Overexpression of *WOR1* in white cells is sufficient to drive mass conversion to the opaque

state, confirming its role as a master switch activator. Conversely, deletion of *WOR1* locks cells in the white state, demonstrating that it is required for opaque identity.

WOR1 functions at the top of a transcriptional cascade that includes additional regulators: *WOR2, WOR3, WOR4, CZF1, EFG1,* and *AHR1*, among others (Zordan et al., 2007; Hernday et al., 2013). *EFG1* acts as a white-state activator and repressor of *WOR1*, while *WOR1* represses *EFG1*, creating a bistable toggle switch architecture. The mutual repression between *WOR1* and *EFG1* underlies the stability of each cell state: once a cell commits to either the white or opaque program, it tends to maintain that state across cell divisions.

Because *WOR1* resides on Chr1 and its expression is highly dosage-sensitive (Huang et al., 2006; Zordan et al., 2007), the copy number of Chr1 directly affects the transcriptional threshold for switching. However, in trisomic strains carrying three copies of Chr1, elevated dosage of other factors may paradoxically suppress switching. This makes Chr1 copy number a tractable 'dosage lever' for studying the quantitative regulation of epigenetic cell fate decisions (Huang et al., 2006; this study).

2.4 Chromosome 1 and Aneuploidy in *C. albicans*

Aneuploidy, the gain or loss of individual chromosomes, is remarkably well-tolerated by *C. albicans*, which differs from most diploid eukaryotes in this respect. Whole-chromosome aneuploidy can arise spontaneously in *C. albicans* isolates, and has been documented in response to antifungal drugs, environmental stress, and during infection (Selmecki et al., 2006; 2010). Rather than being deleterious, aneuploidies are often adaptive, providing reversible phenotypic variation without permanent genetic change.

Chromosome 1 is the largest chromosome in the *C. albicans* genome (~3.15 Mb) and encodes a collection of functionally important genes, including *WOR1*, as well as chromatin regulators (*SET1, HAT1,*

RTT102), transcription factors (*STP2, RIM101, BRG1, TAF145*), and stress response regulators (*IRA2, RPN4, TUP1, HST1, HBR1*). A *C. albicans* WO-1 strain used in this study naturally contains a trisomy of Chr1 (three copies), providing an ideal experimental system to manipulate Chr1 dosage and study its functional consequences. Preliminary observations in the Bennett lab showed that Chr1-aneuploid strains show dramatically reduced white–opaque switching frequencies, while loss of the extra Chr1 copy leads to hyper switching. Critically, Chr1 is intrinsically unstable in the WO-1 background, with spontaneous chromosomal loss events occurring at elevated frequencies. Understanding the specific gene content responsible for this dosage-dependent switching suppression is the central goal of this thesis.

3. Materials and Methods

3.1 Strains and Culture Conditions

All experiments were performed using derivatives of the *Candida albicans* WO-1 strain background (also referred to as "Soll1"), originally obtained from the Soll laboratory (University of Iowa) via the Broad Institute stock (strain CAY 12307). This strain naturally harbors trisomy of Chromosome 1 and is competent for white–opaque switching. Standard strains used for controls included CAY 16438 (euploid, high-switching positive control) and CAY 16801 (Chr1 trisomic, fluorescently marked, low-switching negative control).

Strains were maintained on YPD agar (1% yeast extract, 2% peptone, 2% dextrose, 2% agar) at 30°C. Switching assays were performed on YPD, SCD (synthetic complete dextrose), and Spider media. Antibiotic selection used nourseothricin (clonNAT, 200 μg/mL) for SAT1-containing constructs and hygromycin B (300 μg/mL) for HygR-containing constructs. SAT1 marker excision was performed by growth on a maltose-containing medium, which activates the FLP recombinase system.

3.2 CRISPR/Cas9-Mediated Fluorescent Marker Integration

To enable real-time tracking of Chr1 copy number, fluorescent reporters were integrated into two distinct Chr1 homologs using CRISPR/Cas9 editing. Repair templates were designed containing either the green fluorescent protein mNeonGreen coupled to a *SAT1* selectable marker, or the red fluorescent protein mScarlet coupled to a *HygR* selectable marker. Each template was flanked by ~500 bp homology arms targeting the *TDH3* locus on Chr1, situated proximal to the centromere.

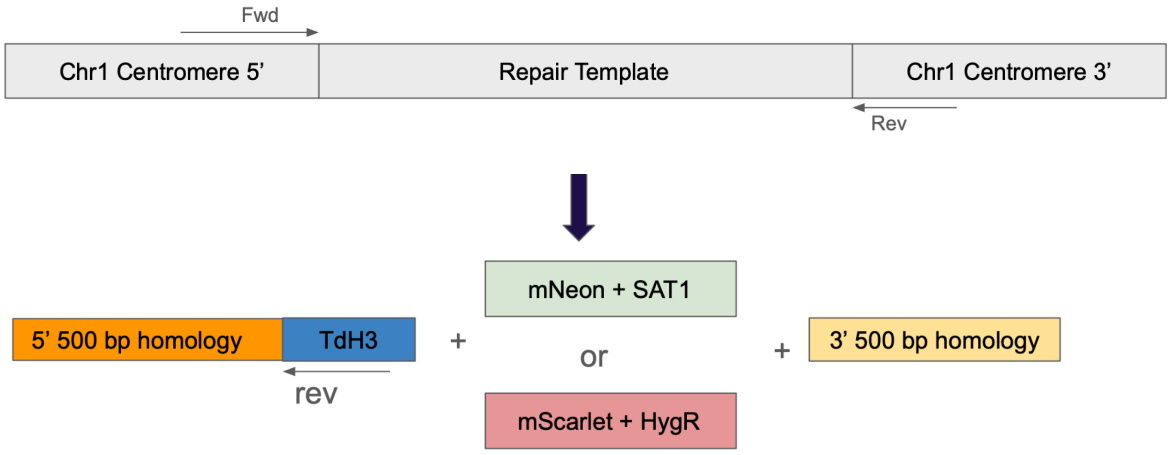

Figure 1. Schematic of fluorescent marker integration at the Chr1 *TDH3* locus. Repair templates containing either mNeonGreen–*SAT1* or mScarlet–*HygR* were flanked by 5' and 3' 500 bp homology arms to direct integration near the centromere by homologous recombination.

Templates were assembled by Phusion PCR and introduced into CAY 12307 along with a CRISPR/Cas9 plasmid encoding a guide RNA targeting integration near the centromere on Chr1. Transformants were selected on antibiotic-containing media, and colonies carrying both fluorescent markers (one mNeonGreen, one mScarlet) were identified by fluorescence microscopy. Integration of each marker at the correct chromosomal locus was confirmed by colony PCR using junction-specific primers

3.3 Segmental Chromosomal Deletion using CRISPR/Cas9 system

To study how different parts of Chromosome 1 affect switching in *Candida albicans*, four segmental deletions were designed spanning both arms of Chr1: DelA, DelB, DelC, and DelD. Each deletion was targeted using two flanking gRNAs, cloned into a CRISPR/Cas9 plasmid by Golden Gate Assembly.

Repair templates consisted of a *SAT1* selectable marker flanked by ~500 bp homology arms matching the sequences immediately flanking each deletion boundary, enabling homologous recombination-mediated replacement of the targeted region.

To make sure the plasmids were built correctly, colony PCR and restriction enzyme digests were used to check the gRNA and repair template inserts in bacteria, and positive clones were confirmed by Sanger sequencing. Once confirmed, the plasmids would be used to transform *Candida albicans*. This approach was designed to remove specific parts of Chromosome 1 and observe how those changes affect chromosome stability and the ability of the cells to switch between white and opaque states.

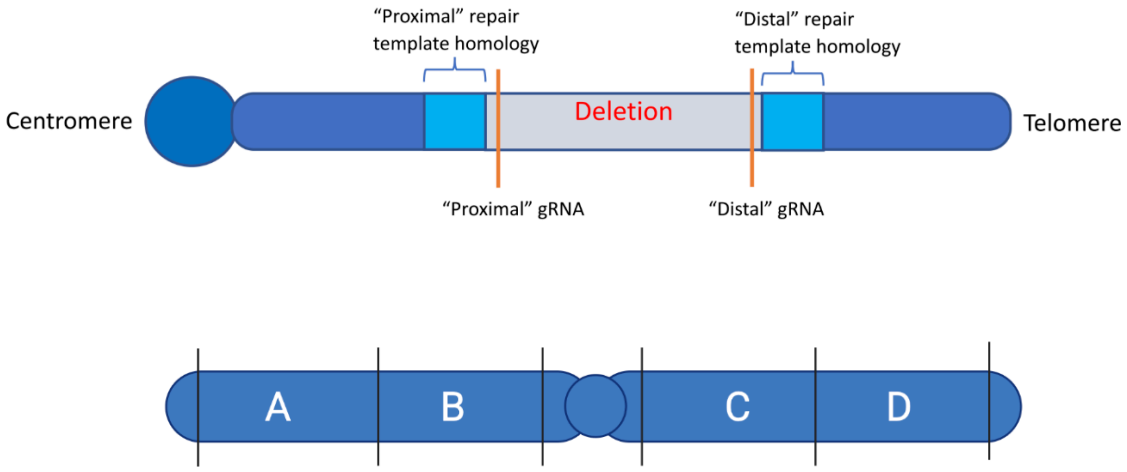

Figure 2. Schematic of CRISPR/Cas9-mediated segmental deletion strategy and Chr1 deletion region map. Top: Diagram illustrating the dual-gRNA approach used to generate each segmental deletion. Two gRNAs targeting flanking sequences on either side of the deletion boundary direct

Cas9 cleavage, and a SAT1-marked repair template with proximal and distal homology arms mediates replacement of the intervening sequence by homologous recombination.

3.4 Gene Knockouts: *TUP1*

Single-copy (heterozygous) knockout of *TUP1* was introduced into the trisomic WO-1 (Soll1) background using *SAT1*-flanked deletion cassettes. The deletion cassette was generated with ~1 kb homology arms; integration was confirmed by 5′ junction PCR (primers 9021/4360, ~1 kb) and 3′ junction PCR (primers 4439/8120, ~1.3 kb). All knockout strains were confirmed by gel electrophoresis and the *SAT1* marker was flipped out by growth on maltose medium before downstream assays.

3.5 White–Opaque Switching Assays

White–opaque switching frequencies were assessed using a standard colony-based switching assay. White cell populations were grown overnight in liquid YPD at 30°C, diluted to approximately 200 cells per 200 µL water, and plated at 100 cells per plate on YPD, SCD, and Spider agar. Plates were incubated at room temperature (~22°C) and examined at 7, 10, and 14 days post-plating.

Colonies were scored for the presence of opaque sectors. Switching frequency was calculated as the percentage of colonies containing at least one visible opaque sector. For strains carrying fluorescent markers, simultaneous fluorescence imaging was performed to correlate switching behavior with the presence or absence of mNeonGreen and mScarlet signals, providing a readout of Chr1 homolog retention.

3.6 Fluorescence Microscopy and Image Analysis

Fluorescence imaging of colony plates and individual cells was performed using a fluorescence stereomicroscope equipped with GFP and RFP filter sets. Single-cell imaging was performed on a widefield fluorescence microscope. Red-to-green fluorescence ratios were calculated from triplicate

images per strain using the automated Python analysis pipeline developed by Jonathan Weiss in the Bennett lab.

3.7 Whole-Genome Sequencing and Coverage Analysis

Genomic DNA was extracted from overnight cultures using a standard glass bead lysis protocol followed by phenol-chloroform extraction and ethanol precipitation. DNA concentrations were measured by Qubit fluorometry. Illumina whole-genome sequencing libraries were prepared and sequenced at 150 bp paired-end. Sequencing reads were aligned to the *C. albicans* SC5314 reference genome (Assembly 22). Coverage analysis and heterozygosity plots were generated by Dannie Yin or Corey Frazer using sliding-window coverage tools and in-house scripts. Coverage plots were visualized in IGV (Integrative Genomics Viewer) to identify regional copy number changes and structural breakpoints. Long-read sequencing (Oxford Nanopore or PacBio) was prepared for four samples (Soll1, Soll2, TUP1 het, Strain 253) at concentrations of 20.8–319 ng/μL.

3.8 Telomere-Mediated Chromosomal Truncation

Telomere-mediated chromosomal truncation was explored as a strategy for progressive dissection of Chr1 region D. The truncation cassette followed the established three-element architecture: **[Chromosomal Mapping Sequence]–[Selectable Marker (SAT1)]–[Telomere Seed]**. The telomere repeat sequence was cloned from pKA05 (*Candida* telomere plasmid) into the pSFS2A backbone (containing the SAT1/FLP recombinase system). The enzyme strategy PstI/XhoI/HindIII was used for pKA05 (generating fragments of ~3300, ~1450, and ~2675 bp) and PstI/XhoI/NcoI-HF for pSFS2A (generating fragments of ~3950, ~1440, and ~1957 bp). Ligation and *E. coli* transformation were performed at 3:1 insert:vector and vector:insert ratios. Correct construct assembly was confirmed by colony PCR and verified by Sanger sequencing.

To generate linear truncation cassettes for *C. albicans* transformation, Phusion PCR was performed on the verified plasmid using long forward primers paired with a common telomere cap reverse primer. Each forward primer carries ~80 bp of chromosomal homology sequence targeting a defined position within the region, followed by a shared plasmid-annealing sequence. By using primers that target progressively more centromere-proximal positions, a series of cassettes was generated that each remove a successively shorter distal chromosomal segment. This design allows systematic dissection of the region at increasing resolution, each cassette tested narrows down the interval responsible for switching suppression. The linear cassettes were transformed into *C. albicans* strains carrying either a deletion of region B or a deletion of region D, allowing the contribution of each region to be assessed independently in the truncation background.

4. Results

4.1 Chr1 Trisomy Suppresses Switching; Chr1 Loss Drives Hyper switching

This project originated from an unexpected observation made during routine switching assays on a panel of WO-1 laboratory strains. Initial switching assays on trisomic (3×Chr1) WO-1 strains revealed that these strains were predominantly non-switchers on YPD at 7 days at room temperature, producing smooth, uniformly white colonies with only 3–5% switching to opaque observed. Interestingly, however, scattered sectors of subtly different colony morphology were also visible within these otherwise non-switching colonies. *(Following observations and data were made my previous Bennett lab member)*

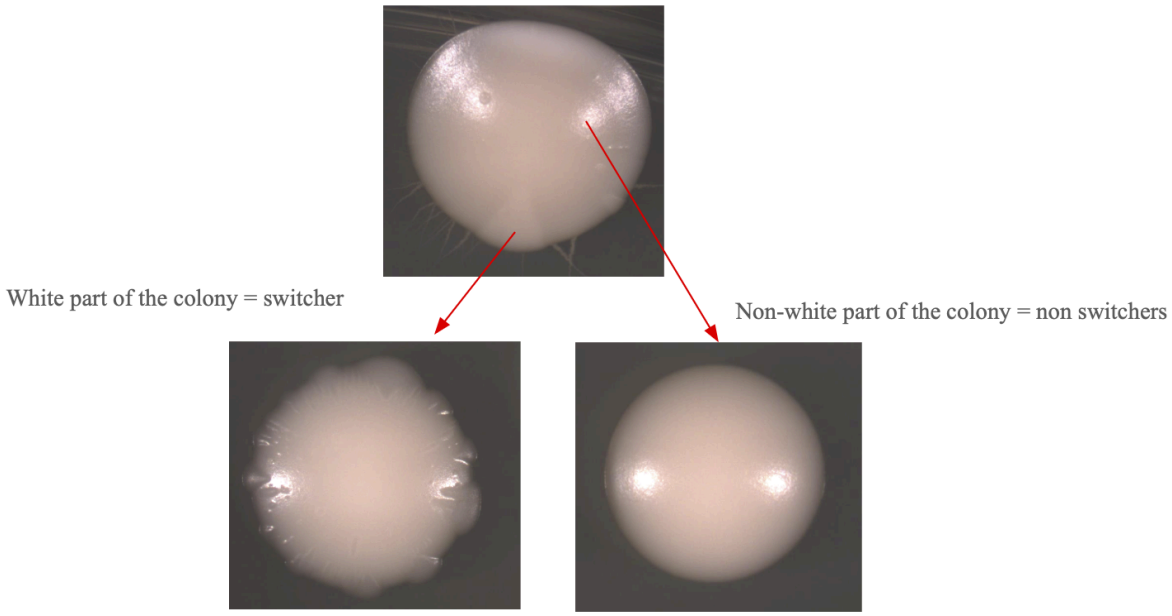

Figure 3. Colony morphology of the WO-1 Soll1 strain showing rare high-switching sectors. Representative images show isolates grown on YPD at 7 days (22°C). Sectors of subtly different morphology are visible within individual colonies and were isolated for downstream analysis.

To investigate the nature of "extra white" sectors, cells were taken from the bulk part of the sector or from the "extra white" sector. When these isolates were re-plated in switching assays, the pattern was unambiguous: all sector-derived isolates showed high levels of white-to-opaque switching (90–100%), while all bulk colony isolates showed only low-level switching (3–5%). Switching frequency was scored manually by visual inspection under a fluorescence stereomicroscope, with 100–150 colonies scored per plate across three independent biological replicates per condition.

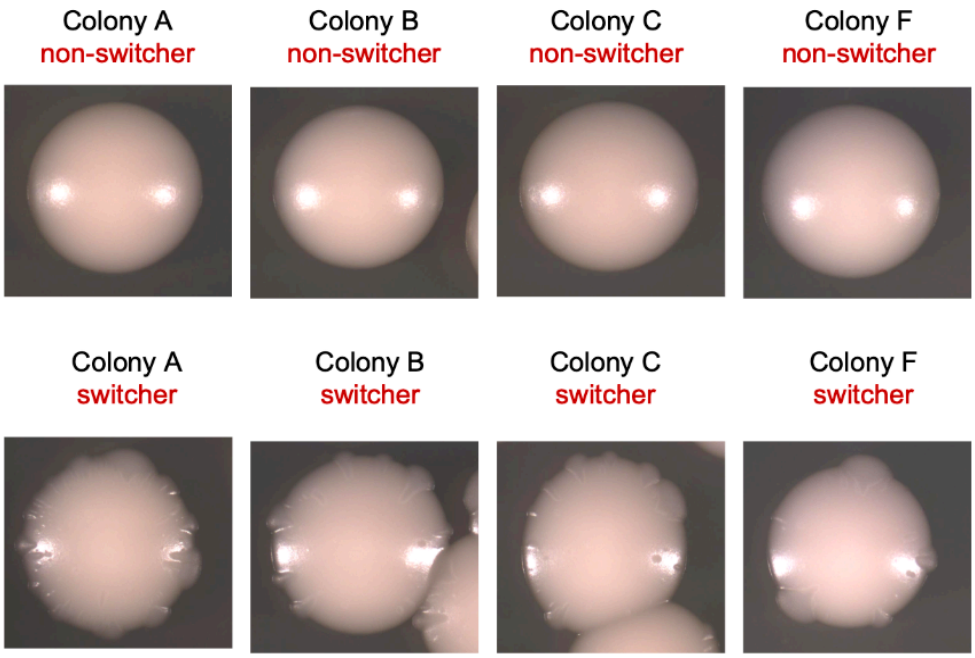

Figure 4. Switching frequency of sector-derived isolates from sectored WO-1 colonies. Colony images (left) show representative non-switcher (top row) and switcher (bottom row) morphologies for four independently isolated colonies (A, B, C, F) grown on YPD at 22°C for 7 days. Non-switchers produce smooth, uniformly white colonies; switchers display characteristic rough, sectored morphology.

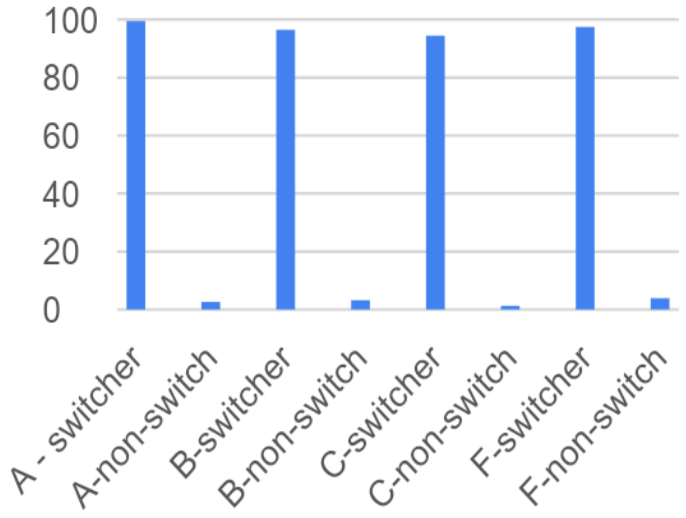

Figure 5. The bar graph (right) shows switching frequency (%) for each isolated pair. Switching frequency was scored manually by visual inspection under a fluorescence stereomicroscope; 100–150 colonies per plate, n = 3 biological replicates per condition.

Whole-genome sequencing of parental and “extra white” colonies revealed that the whiter sector-derived cells had lost the extra copy of Chr1, reverting from trisomy to disomy for this chromosome. In contrast, the parental (low-switcher) cells had retained the trisomic Chr1 configuration. This one-to-one correspondence between Chr1 copy number and switching competence, observed across all three independently picked colonies, established a direct link between Chr1 dosage and the frequency of white–opaque switching.

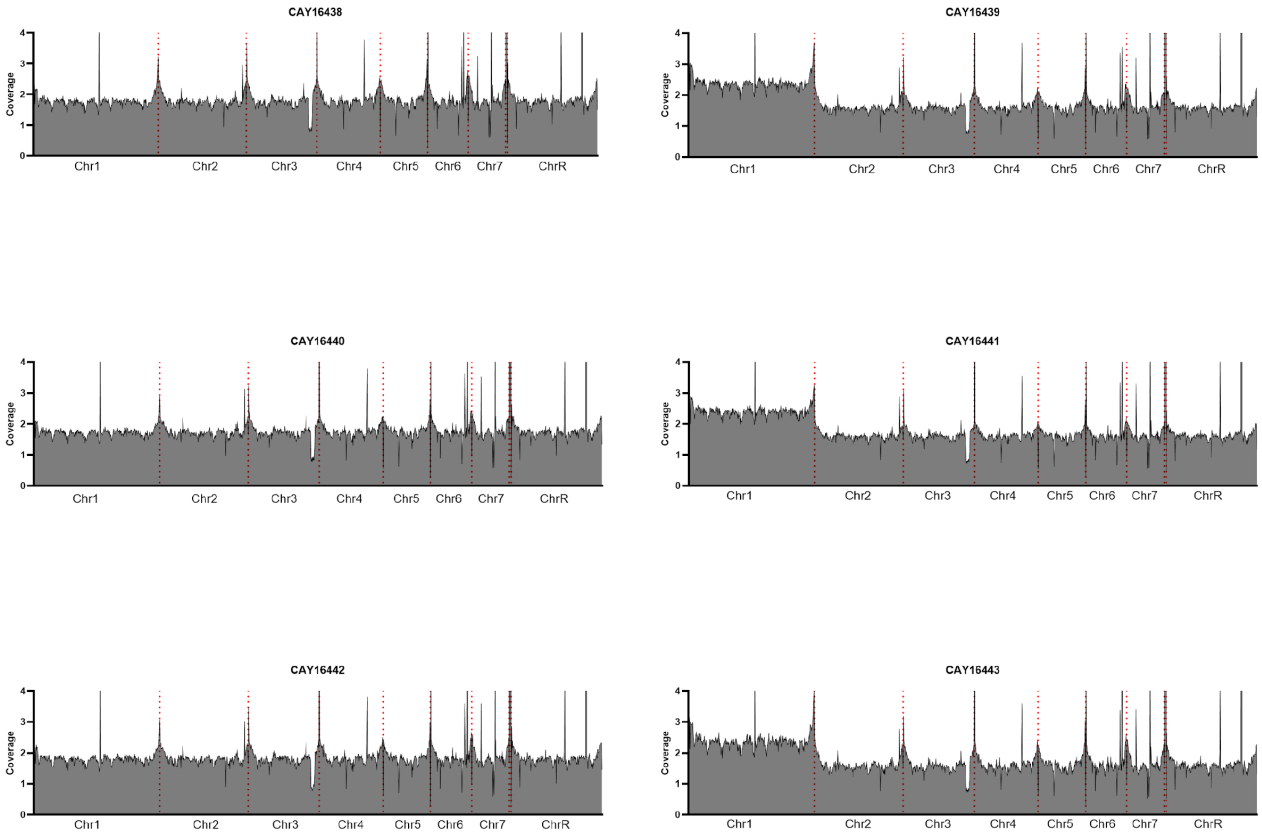

Figure 5. Chr1 loss drives hyperswitching. WGS coverage plots for six isolates derived from three sectored colonies, three from high-switching sectors and three from the paired low-switching bulk colony. High-switching isolates show loss of the extra Chr1 copy (trisomy to disomy), while low-switching isolates retained trisomy. Switching phenotype is indicated for each isolate.

This result was unexpected as *WOR1*, the master activator of white-to-opaque switching, is itself located on Chr1. Thus, the initial expectation was that trisomic strains carrying three copies of Chr1 would switch more than disomic strains. The observation that the opposite was true suggested that dosage-sensitive opaque repressors must also reside on Chr1, and that their increased dosage in the trisomic state outweighs the additional *WOR1* copy, resulting in net suppression of switching. This is consistent with a prior study that directly manipulated *WOR1* copy number in WO-1, demonstrating that progressive deletion of *WOR1* copies reduced switching under anaerobic conditions on Lee's medium

(Ramírez-Zavala et al., 2008). Importantly, that study deleted only *WOR1* in isolation, leaving all other Chr1 genes at normal dosage. In our system, the entire Chr1 is trisomic, meaning repressor genes are also present at elevated copy number alongside *WOR1*. The net suppression of switching we observe therefore reflects the combined dosage of multiple Chr1-encoded repressors rather than *WOR1* alone.

4.2 Fluorescent Markers Enable Live Tracking of Chr1 Copy Number

To enable monitoring of Chr1 copy number dynamics in live cells, fluorescent markers were integrated into distinct Chr1 homologs in the trisomic WO-1 background. Using CRISPR/Cas9-mediated editing, mNeonGreen (green) was integrated into one Chr1 homolog and mScarlet (red) into another under the strong pTDH3 promoter and introduced near the centromere. The resulting strain carried a 2G:1R Chr1 configuration (two green-marked and one red-marked Chr1 copy). Colony PCR was done for marker integration confirmation using junction-specific primers demonstrated correct 5′ and 3′ integration of both markers in the selected strains.

To validate fluorescent marker integration and confirm Chr1 copy number, colonies were imaged using a Zeiss fluorescence microscope with fixed imaging parameters maintained across all imaging sessions. Because mScarlet and mNeonGreen differ in their detection properties under these conditions, a control strain carrying one copy of each fluorescent marker (1R:1G) was included to establish an empirical normalization baseline. Experimental R/G ratios were normalized to this control value, such that deviations below 1.0 indicate proportionally more green than red signal. Both colony 1 and colony 19 produced normalized ratios below 1.0, confirming the expected 1R:2G trisomic Chr1 configuration.

A.

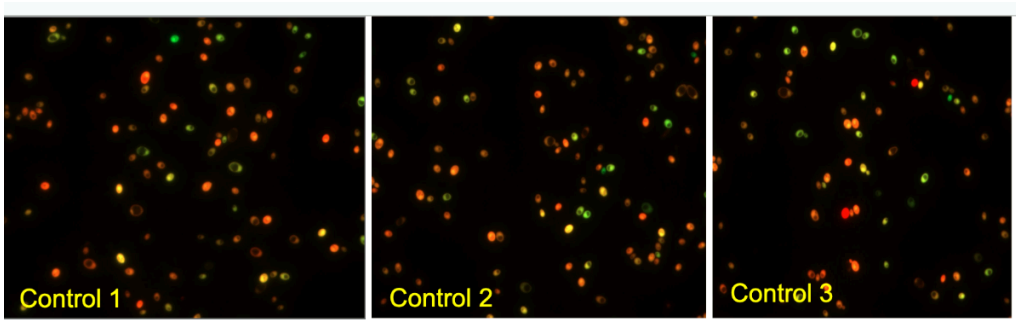

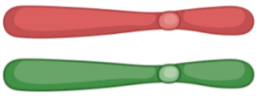

Image	Average Red/Green Ratio
control.1	1.84
control.2	2.03
control.3	1.96
Average Control	1.94
AVc/AVc	1

B.

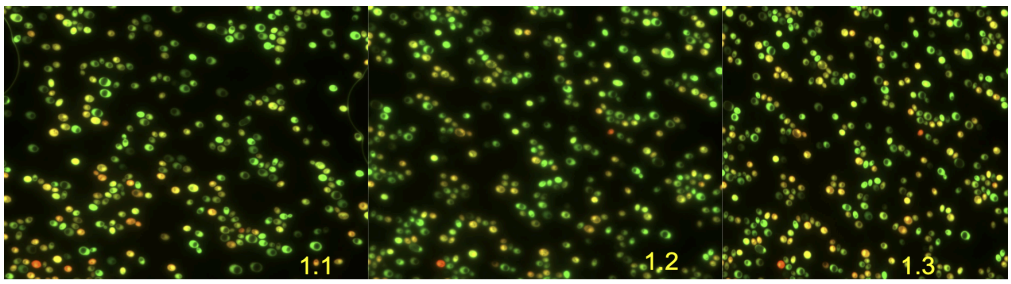

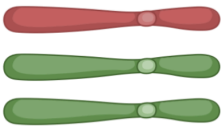

Image	Average Red/Green Ratio
1.1	0.71
1.2	0.61
1.3	0.67
Average value - AV1	0.67
AV1 / AV control	0.34

C.

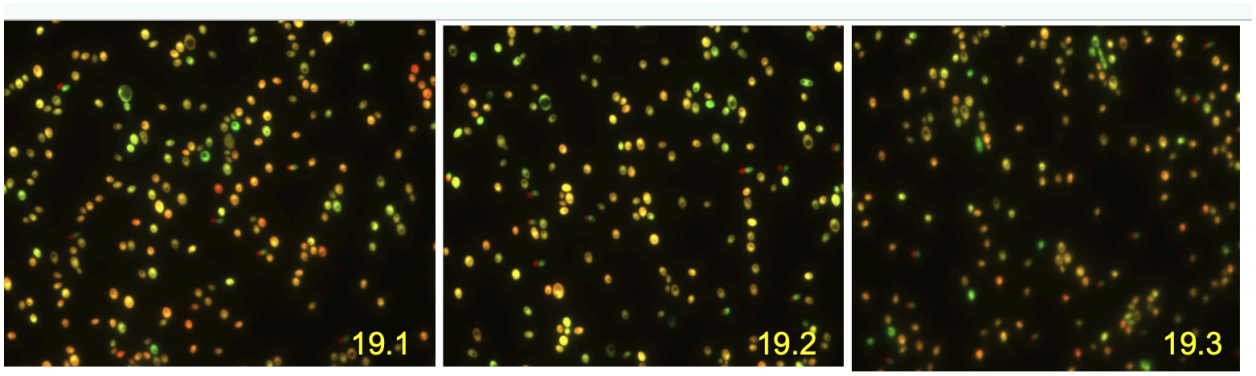

Image	Average Red/Green Ratio
19.1	0.73
19.2	0.63
19.3	0.71
Average value - AV19	0.69
AV19 / AV control	0.35

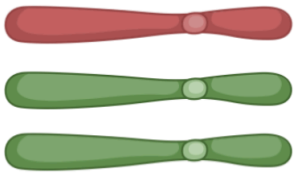

Figure 6. Fluorescent marker quantification confirms trisomic Chr1 configuration. Fluorescence microscopy images of colonies carrying mScarlet (red) and mNeonGreen (green) markers integrated on distinct Chr1 homologs. Three independent images were acquired per colony under fixed imaging parameters. Chromosome configurations are depicted schematically alongside each dataset (red and green bars represent mScarlet- and mNeonGreen-marked Chr1 homologs respectively). **(A)** Control strain carrying one mScarlet-marked and one mNeonGreen-marked Chr1 homolog (1R:1G). Average Red/Green (R/G) fluorescence intensity ratio = 1.94, establishing the normalization baseline (AVc). **(B)** Colony 1 images 1.1–1.3. Average R/G = 0.67; normalized to AVc = 0.34, consistent with 1R:2G trisomic configuration. **(C)**Colony 19 images 19.1–19.3. Average R/G = 1.24; normalized to AVc = 0.64, consistent with 1R:2G trisomic configuration.

Whole-genome sequencing of the engineered strains demonstrated elevated Chr1 read depth consistent with trisomy, and heterozygosity plots (generated by Dannie Yin) showed the expected SNP distribution across all chromosomes. Mapping of fluorescent marker sequences confirmed integration of both mNeon (178 mapped reads in KM_14; 326 in KM_15) and mScarlet (90 and 104 mapped reads, respectively) at the intended chromosomal loci. These validated reporter strains enabled subsequent experiments in this study.

Whole genome coverage plot:

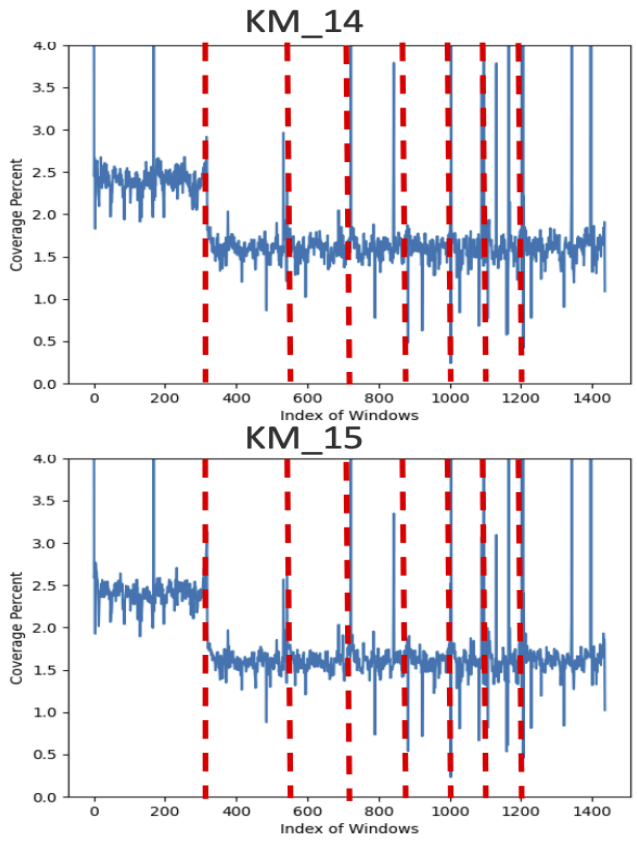

Raw Heterozygosity plot:

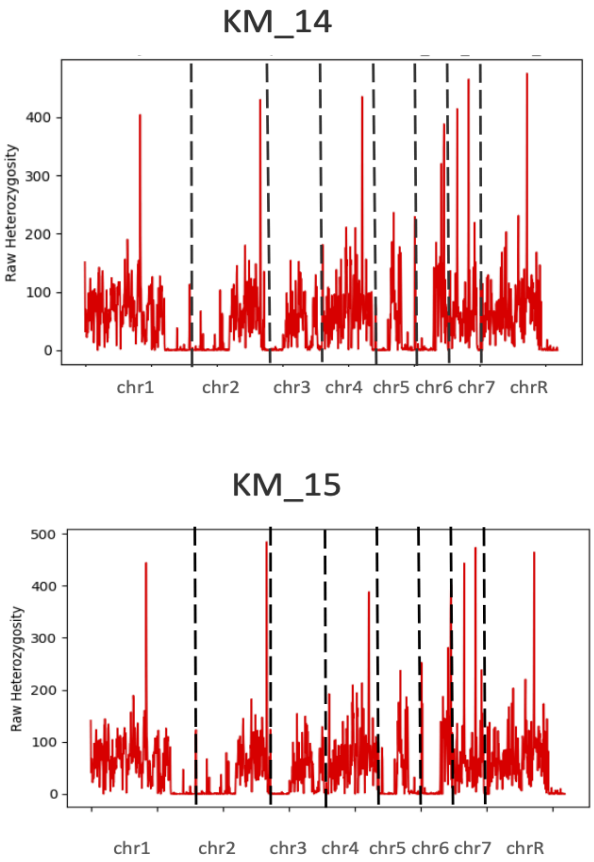

KM_RFP/GFP1	Length(bp)	Mapped	Unmapped
mNeon	711	**178**	0
mScarlet	696	**90**	0
*	0	0	51604

KM_RFP/GFP2	Length(bp)	Mapped	Unmapped
mNeon	711	**326**	0
mScarlet	696	**104**	0
*	0	0	83642

Figure 7. Whole-genome sequencing confirms Chr1 trisomy and marker integration in engineered strains KM_14 and KM_15. Left: Coverage depth plot showing elevated Chr1 read depth (~1.5× relative to other chromosomes). Right: Raw heterozygosity plot showing SNP distribution across all chromosomes, consistent with trisomy. Coverage analysis and plots generated by Dannie Yin.

4.3 *TUP1* Heterozygous Knockout Produces Variable Switching Outcomes

TUP1 encodes a general transcriptional corepressor with well-characterized roles in repressing filamentation and influencing phenotypic switching pathways in *C. albicans* (Braun & Johnson, 1997). Because *TUP1* was identified as a candidate switching suppressor in region D, we generated single-copy (heterozygous) knockouts of *TUP1* in the trisomic WO-1 background. PCR screening identified colonies 7, 9, and 15 as successful *TUP1* heterozygous knockouts (CAY 16661 and CAY 16720, among others), confirmed by both 5′ and 3′ junction PCR.

Switching assays on confirmed *TUP1* het KO colonies revealed variable and mixed behavior. Some transformants (e.g., CAY 16720) displayed a hyper-switching phenotype comparable to full Chr1 loss, while others (e.g., CAY 16661) showed similar switching to the parental strain. This heterogeneity suggested that reducing *TUP1* dosage by one copy is not consistently sufficient to drive switching on its own.

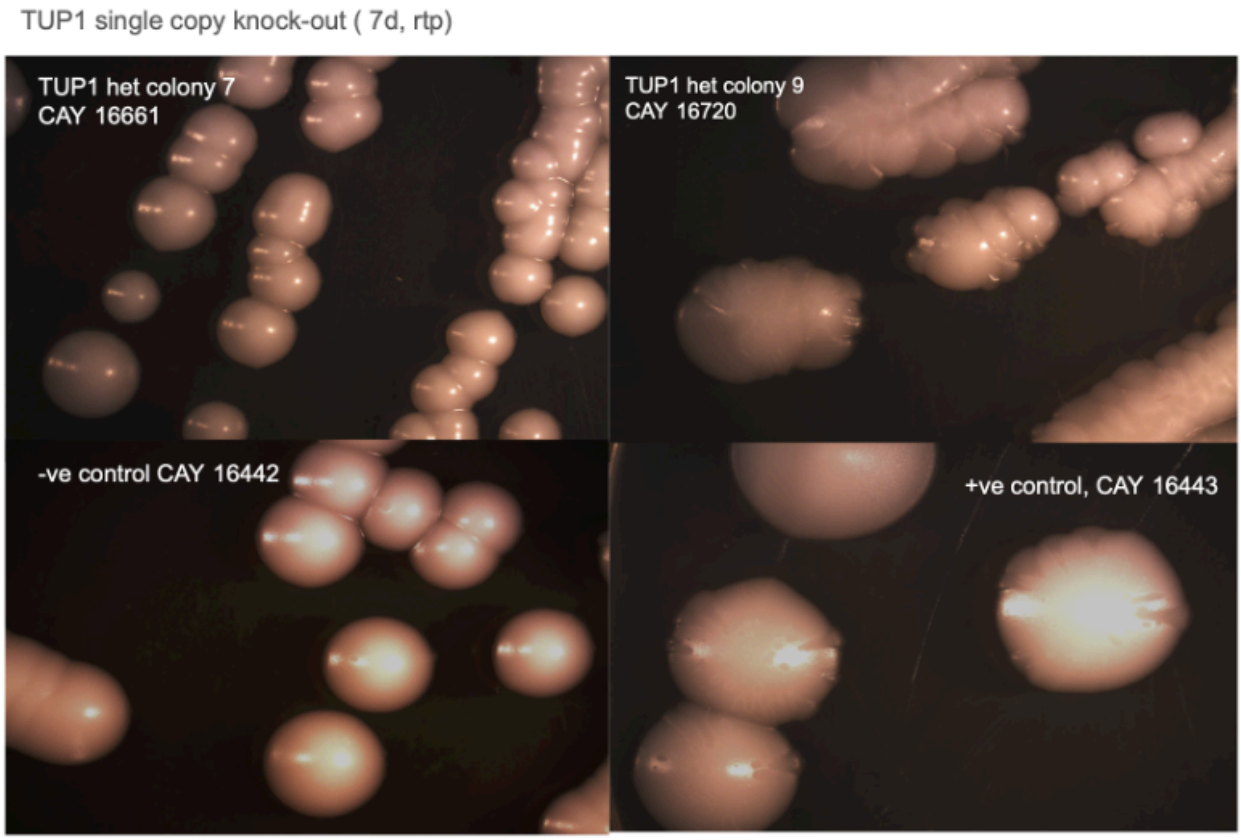

Figure 8. Variable switching phenotypes in *TUP1* het knockout colonies. Switching assay results showing hyper-switching in CAY 16720 and no increase in CAY 16661.

** Representative brightfield microscopy images showing colony morphology at higher magnification. Images are shown for qualitative comparison of phenotype and are not to scale.*

To investigate this, whole-genome sequencing and coverage analysis was performed on the hyper-switching *TUP1* het strain (CAY 16720). Coverage analysis revealed a sharp drop in read depth along Chr1 beginning at approximately 890,000 bp, with the likely breakpoint pinpointed by IGV analysis to exactly 890,460 bp. This coverage drop indicates loss of a portion of Chr1 in the hyper-switching strain, a structural event not present in a low-switching *TUP1* het strain (CAY 16661), which showed normal uniform Chr1 coverage (Figure 9). These data indicate that the hyper-switching phenotype in CAY 16720 is likely attributable to loss of a large part of Chr1 rather than to heterozygosity of *TUP1* per se.

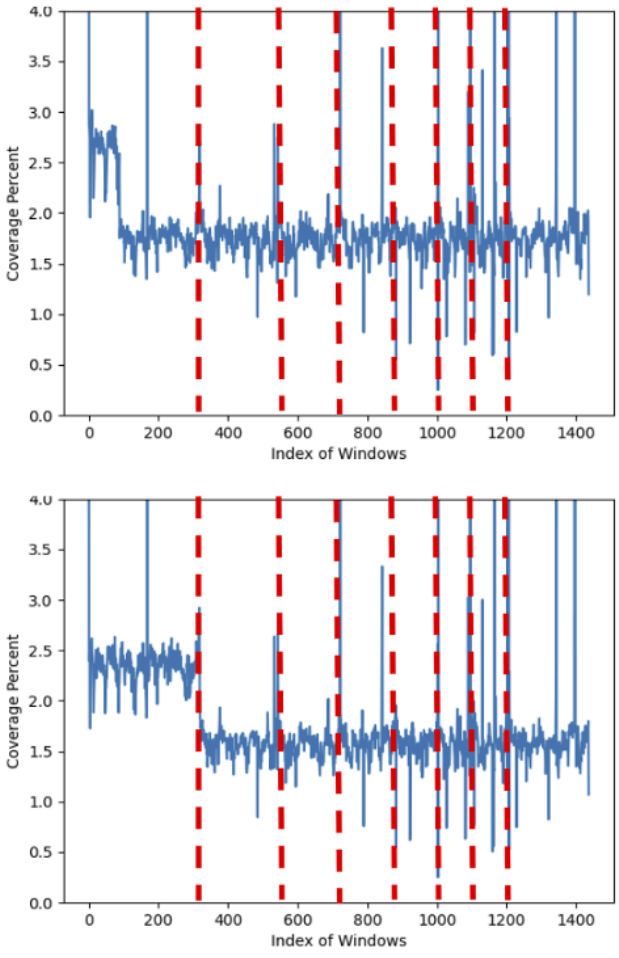

Figure 9. Chr1 arm loss in the hyperswitching *TUP1* het strain. Coverage plots for CAY 16720 (hyperswitcher, top) and CAY 16661 (non-switcher, bottom). CAY 16720 shows a sharp drop in read depth beginning at ~890,000 bp, breakpoint at 890,460 bp by IGV analysis. CAY 16661 shows uniform Chr1 coverage. Analysis by Dannie Yin.

4.4 Segmental Deletions Identify Regions B and D as Switching Modulators

To map regions of Chr1 responsible for switching suppression, CRISPR/Cas9-mediated segmental deletions of four distinct regions were generated in the WO-1 background. The four deletion regions were defined as: DelA (left arm, proximal to the telomere), DelB (left arm, between A and the centromere), DelC (right arm, proximal to the centromere), and DelD (right arm, distal toward the telomere). Each deletion was generated using a dual-gRNA approach with a SAT1 repair template.

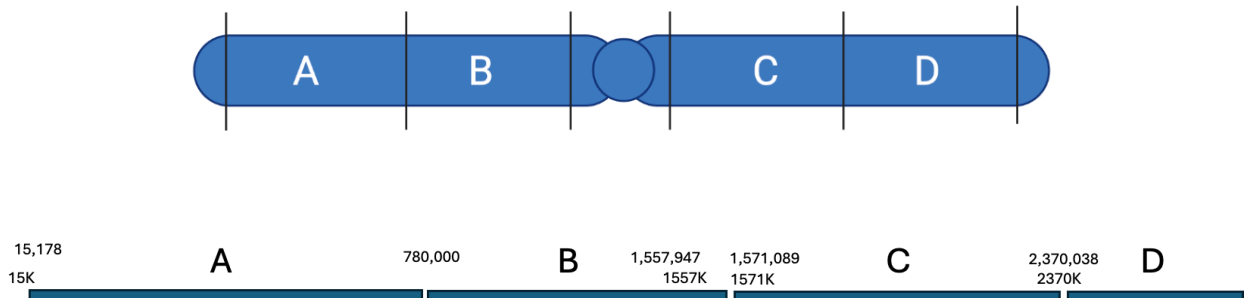

Figure 10. Top: Schematic of Chromosome 1 showing the four segmental deletion regions (A, B, C, D) defined relative to the centromere (filled circle). Regions A and B are located on the left arm; regions C and D are located on the right arm. Bottom: Chromosomal coordinate map of Chr1 showing the approximate genomic positions of each deletion boundary. Region A spans approximately 15,178–780,000 bp; Region B spans approximately 780,000–1,557,947 bp; Region C spans approximately 1,571,089–2,370,038 bp; Region D extends from approximately 2,370,038 bp toward the telomere.

All four segmental deletions were successfully generated in the Soll1 WO-1 background, confirming the feasibility of CRISPR-based segmental engineering of Chr1 at this scale. Representative verified deletion strains include DelA_35 and DelA_36, DelB_9 and DelB_10, DelC_20, and DelD_15 and DelD_30, as confirmed by coverage analysis showing the expected read-depth dropout at the deleted region on one Chr1 homolog.

These strains were made by Dr. Richard Bennett in the lab.

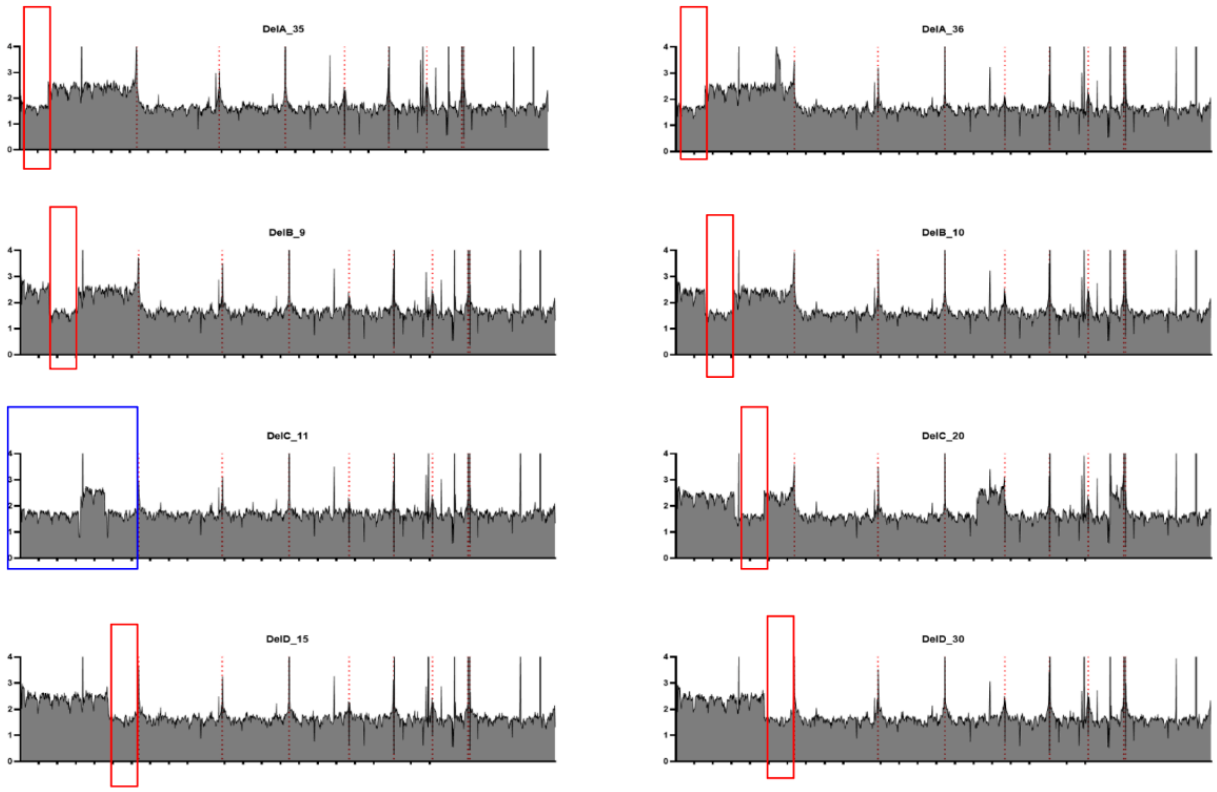

Figure 11. Whole-genome sequencing coverage plots confirming segmental deletions in verified Chr1 deletion strains. Each panel shows read-depth coverage across Chr1 for an individual strain, with the targeted deletion region highlighted by a red box indicating the expected read-depth dropout on one Chr1 homolog. Row 1: region A deletions; Row 2: region B deletions; Row 3: region C deletions; Row 4: region D deletions. Deletion C (blue box, Row 3) shows an extended coverage dropout spanning well beyond the intended deletion boundary, indicating spontaneous large-scale Chr1 loss. Coverage analysis performed by Dannie Yin.

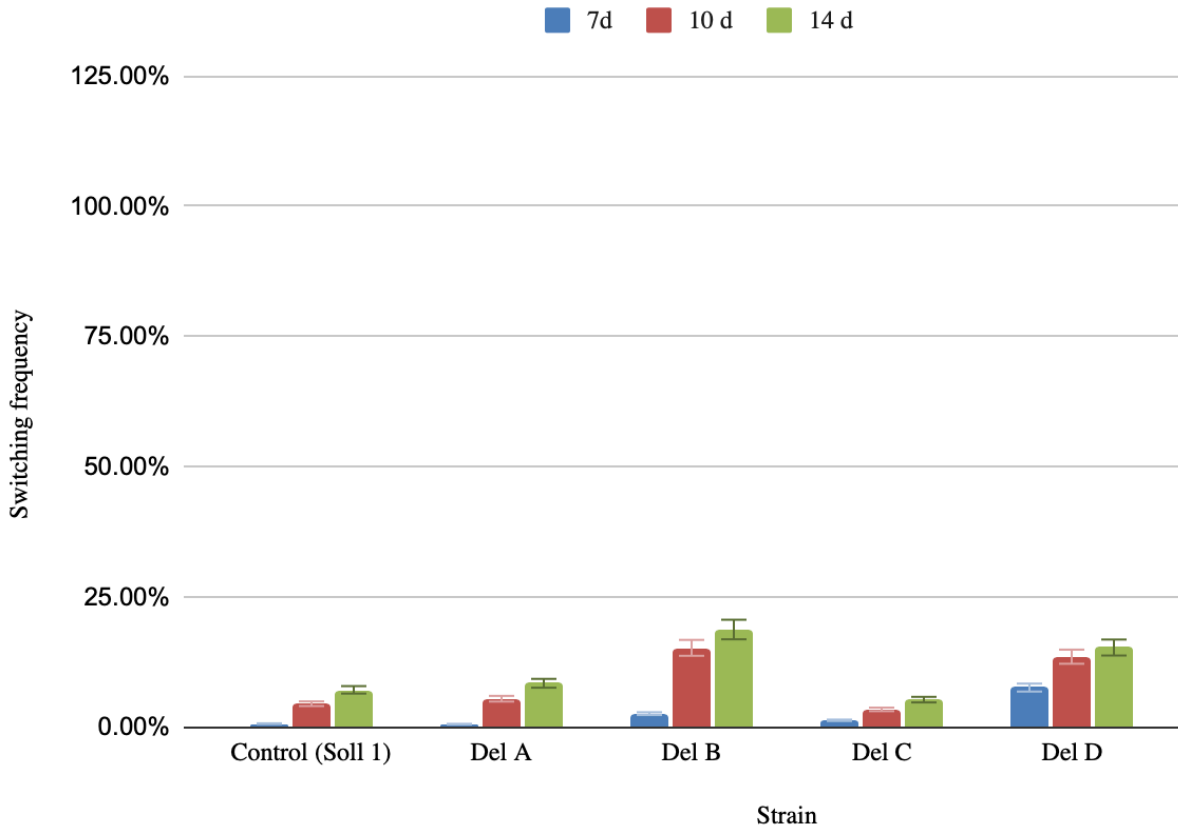

Figure 12. Switching frequencies for single segmental deletion strains. Bar graph showing the percentage of colonies containing at least one opaque sector at 7 days (blue), 10 days (red), and 14 days (green) post-plating for the trisomic control (Soll1), DelA, DelB, DelC, DelD, and DelC #11 strains. DelA and DelC strains show minimal increases over the trisomic control. DelB and DelD strains show moderate, reproducible increases in switching frequency. Switching frequency was scored manually by visual inspection under a fluorescence stereomicroscope; 100–150 colonies per plate.

These results identified regions B and D as the two Chr1 segments harboring the most functionally significant switching suppressors, motivating their combined deletion in the following experiment.

4.5 Combined B+D Deletion Causes Hyper-switching

Given that single deletions of regions B or D each produced moderate switching increases, we hypothesized that their combined loss would phenocopy the hyper switching caused by full Chr1 loss. Multiple B+D double-deletion strains were generated by sequential CRISPR transformation.

Several strains were successfully generated lacking regions B and D in the Soll1 WO-1 strain background. Switching assays on a B+D delete strain (BD19) demonstrated a hyper-switching phenotype, with switching frequencies approaching those observed upon full Chr1 loss. This is the strongest clean genetic result of this study: it demonstrates that the combined gene content of regions B and D is sufficient to account for the switching suppression conferred by the entire Chr1 trisomy, without requiring deletion of regions A, C, or the rest of the chromosome.

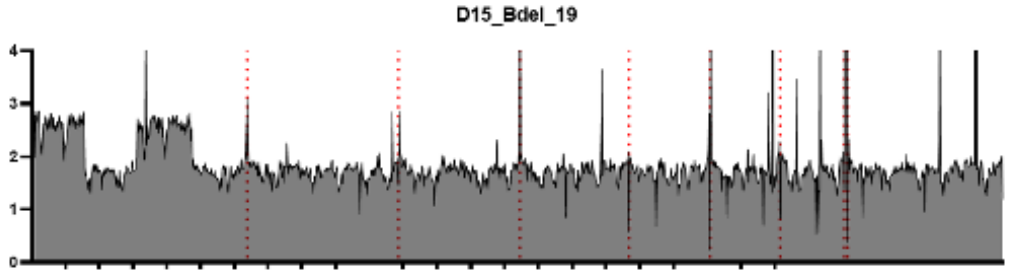

Figure 13. WGS coverage confirms clean B+D double deletion in strain, BD19. Coverage plot shows read-depth dropout at both region B and region D on a single Chr1 homolog, with no additional unintended rearrangements detected.

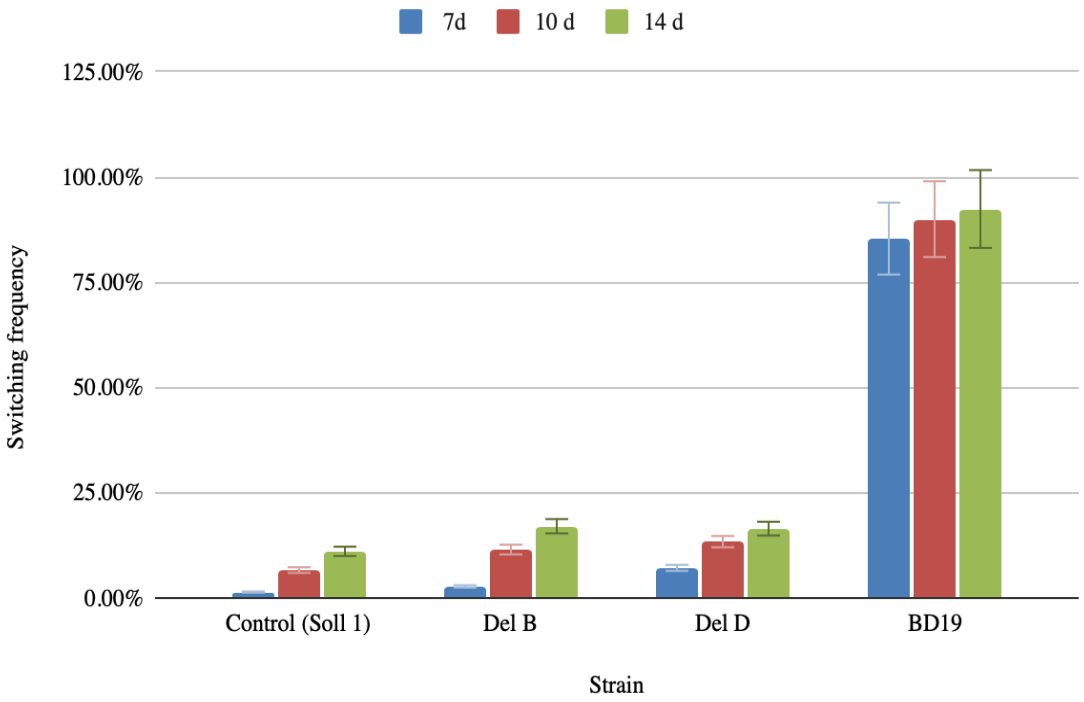

Figure 14. Bar graph showing switching frequencies at 7 days (blue), 10 days (red), and 14 days (green) for the trisomic control (Soll1), DelB, DelD, and BD19. BD19 shows hyperswitching frequencies of approximately 80–95% across timepoints, while single deletion strains show only moderate increases. 100–150 colonies per plate.

Because no single region deletion fully phenocopied the double deletion, the data support a model where multiple dosage-sensitive repressors act together across regions B and D. Chr1 therefore encodes a distributed suppression network rather than a single master repressor, making the system robust to individual gene loss but sensitive to combined dosage reduction.

4.6 Telomere-Mediated Truncation: Construct Development

Segmental deletions of regions B and D demonstrated that the dosage of these two regions, particularly in combination, controls white–opaque switching frequencies. However, these deletions do not reveal which specific genes within these regions are responsible. Both regions span large chromosomal intervals encoding multiple candidate repressors, necessitating a higher-resolution dissection strategy.

To map the genes responsible for switching suppression, we developed a telomere-mediated chromosomal truncation approach. Rather than deleting defined internal segments, this strategy inserts an artificial telomere seed at a defined chromosomal position, which caps the chromosome end at that point and causes loss of all sequence distal to the insertion site. By performing this at progressively more centromere-proximal positions within region D, in a ΔB background where region D's contribution to switching is fully unmasked, we can systematically shrink region D from the distal end inward. Switching assays at each truncation point then identify where the suppressive activity resides, providing much higher resolution than segmental deletions without requiring new CRISPR constructs for every sub-interval.

The truncation cassette consists of three functional components: a chromosomal homology arm that targets integration to a defined position by homologous recombination, a SAT1 selectable marker for transformant selection, and a telomere seed sequence that caps the newly truncated chromosome end. To build this cassette, the telomere repeat sequence was cloned from pKA05 into the pSFS2A backbone containing the SAT1/FLP recombinase system. Linear truncation cassettes were then generated by Phusion PCR, using long forward primers carrying approximately 80 bp of chromosomal homology targeting progressively more centromere-proximal positions within region D, paired with a common telomere cap reverse primer. This design produces a series of cassettes that each remove a successively shorter distal chromosomal segment, enabling systematic dissection of the region at increasing resolution.

This approach is being applied in two complementary configurations: D truncation in a ΔB background, where the truncation cassette is inserted at progressively centromere-proximal positions within region D to identify the minimal suppressive sub-interval of D; and B truncation in a ΔD background, where the analogous strategy is applied to region B. Together, these two truncation series will define the minimal intervals within each region required for switching suppression, and ultimately narrow the search to individual candidate genes for functional follow-up.

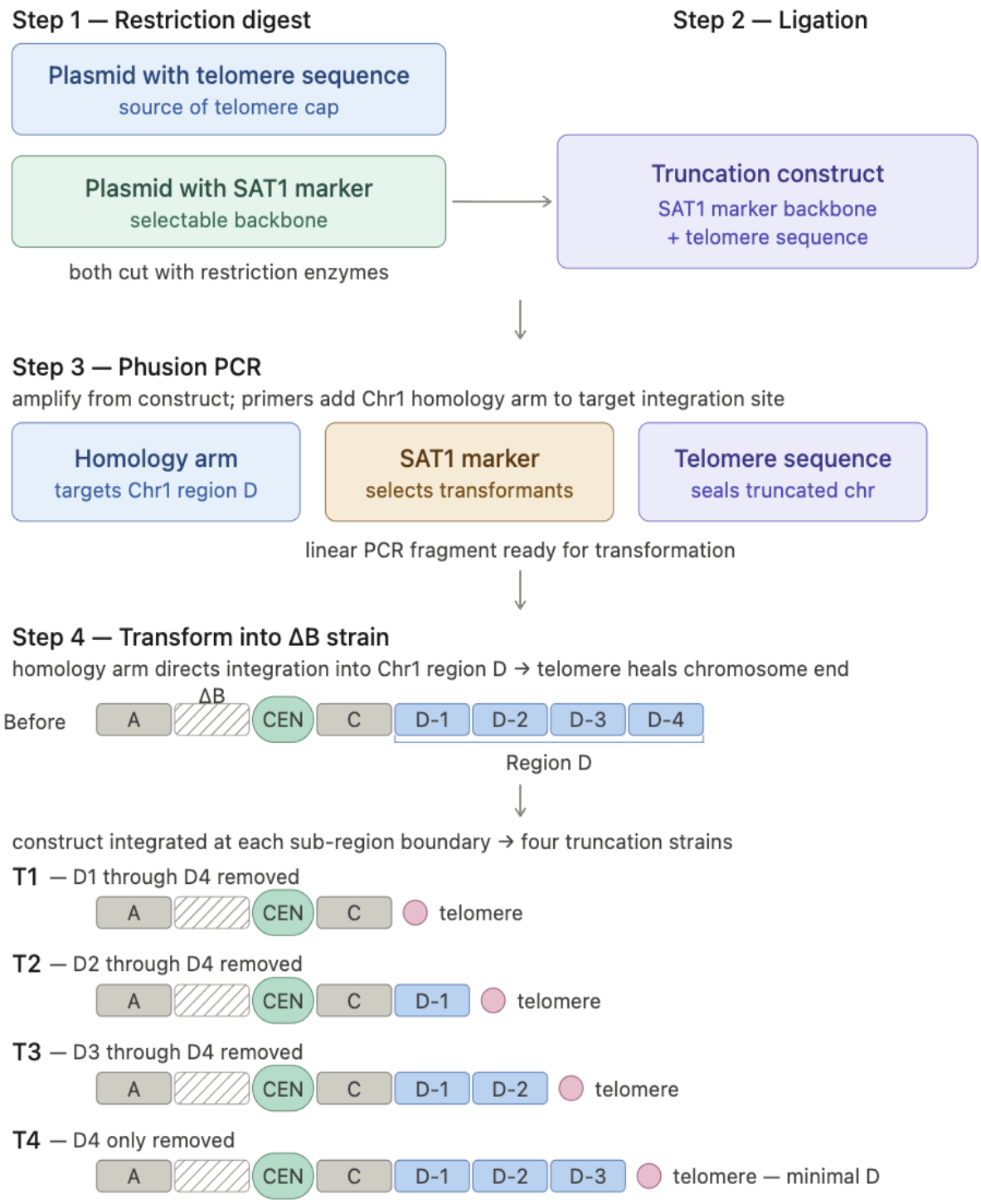

Figure 15. Truncation cassette assembly and progressive truncation of region D. Steps 1–2: Restriction digestion of the telomere-containing plasmid (pKA05) and SAT1 marker backbone (pSFS2A), followed by ligation to generate the truncation construct. Step 3: Phusion PCR appends an ~80 bp Chr1 homology arm to produce a linear cassette comprising three elements: homology arm (targets Chr1 region D), SAT1 marker (selects transformants), and telomere sequence (seals truncated chromosome end). Step 4:

Transformation into the ΔB strain, where the cassette integrates into region D at progressively centromere-proximal positions, generating four truncation strains: T1 (all of region D removed), T2 (D-1 retained), T3 (D-1 and D-2 retained), and T4 (D-1 through D-3 retained; minimal D). Pink circles represent the artificial telomere cap.

Figure 16. Overview of the two complementary telomere-mediated truncation strategies. Building on the detailed D truncation scheme shown in Figure 15, this schematic summarizes both truncation series side by side for clarity. Top (blue): D truncation in a ΔB background. Bottom (purple): B truncation in a ΔD background, where the same cassette logic is applied to region B. Together, these two series will define the minimal suppressive interval within each region. Hatched regions indicate deletions; colored circles represent the artificial telomere cap.

The linear truncation cassette is currently being transformed into *C. albicans* Soll1 WO-1 lacking region B. Successful integration at target sites within region D will be selected on nourseothricin-containing media and confirmed by junction PCR and whole-genome sequencing, which will verify both correct insertion and loss of the distal chromosomal sequence. Switching assays on confirmed truncation strains will then define the minimal sub-interval within region D required for switching suppression, narrowing the list of candidate regulatory genes for future functional analysis.

5. Discussion

5.1 Chr1 Dosage as a Regulatory Lever for White–Opaque Switching

The central finding of this thesis is that the copy number of Chromosome 1 is a powerful, quantitative regulator of white–opaque switching in *Candida albicans*. The dosage-dependent suppression of switching by Chr1 trisomy represents a form of genetic buffering: additional copies of Chr1-encoded repressors raise the transcriptional threshold required to activate the opaque program. Conversely, when Chr1 copy number drops, either through natural aneuploidy or through engineered deletion, the repressive dosage falls below threshold, liberating the positive feedback circuit centered on *WOR1* and enabling higher switching frequencies.

This model is consistent with the quantitative biology of bistable switches. Dosage-sensitive transcription factors acting within positive-feedback circuits create threshold behaviors where small changes in factor concentration can flip cells between stable states. The *WOR1*/*EFG1* toggle switch in *C. albicans* is an experimentally validated bistable system (Lohse & Johnson, 2009; Zordan et al., 2007), and our data indicate that Chr1 gene dosage, particularly from regions B and D, sets the effective repression threshold that determines which state prevails.

5.2 Regions B and D Encode a Distributed Switching Suppression Network

Regions B and D are the functionally dominant Chr1 segments for switching suppression. The moderate switching phenotypes of single ΔB or ΔD strains, compared to the robust hyperswitching of the BD double deletion strains, indicate that regions B and D make partially redundant contributions to the overall suppressive dosage. This redundancy explains why full Chr1 loss (which removes all four regions) produces such strong phenotypes: it removes both redundant suppressor pools simultaneously.

Regions B and D together encode multiple known transcriptional repressors and chromatin regulators including *RPN4, HAT1, SET1, OFR1, EAF6, LYS143, STP2, RIM101, IRA2, RTT102, TAF145,* and

BRG1, suggesting that the combined dosage of multiple repressor activities, rather than any single gene, underlies the observed switching suppression.

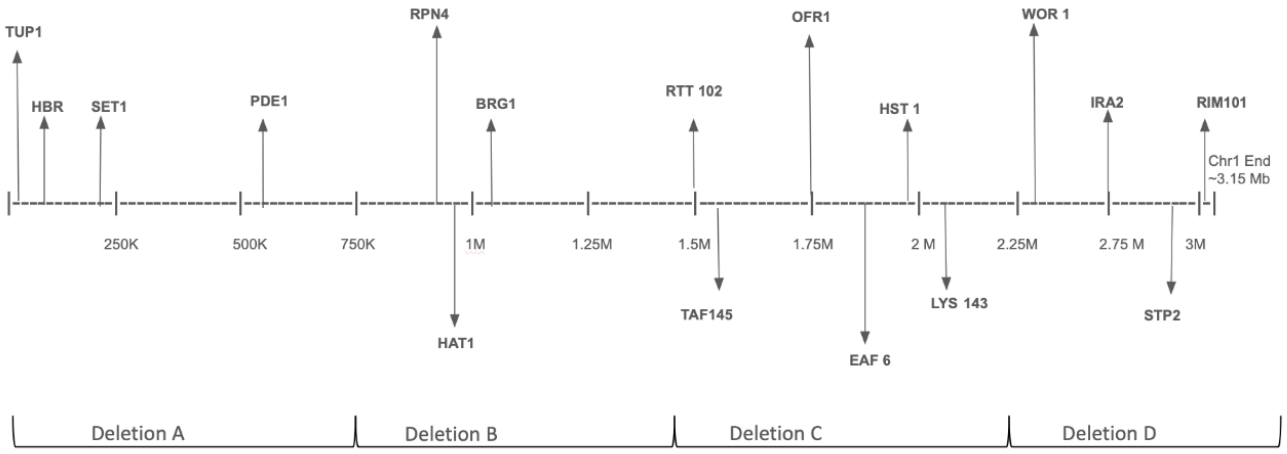

Figure 17. Chromosomal map of *C. albicans* Chr1 showing the positions of key candidate regulatory genes relative to the four segmental deletion regions. Genes are plotted at their approximate genomic coordinates along Chr1 (~3.15 Mb).

Among these candidates, several stand out based on their documented roles in regulating white–opaque switching. *SET1* (region B) encodes a histone H3K4 methyltransferase that directly influences switching frequency in *C. albicans*; deletion of *SET1* increases white-to-opaque switching, suggesting that in the trisomic background, extra copies of *SET1* raise the epigenetic barrier to *WOR1* activation (Raman et al., 2006; Hnisz et al., 2010; Qasim et al., 2021). *TUP1* (region D) is a well-characterized general corepressor with documented roles in repressing opaque-specific gene expression (Braun & Johnson, 1997). Although heterozygous knockout of *TUP1* alone was insufficient to drive switching in our trisomic background, this is consistent with the distributed suppression model, *TUP1* likely acts in concert with other repressors rather than as a sole gatekeeper. *RIM101* (region D) is a transcription factor with documented influence on white–opaque switching; a systematic genetic screen identified Rim101 as capable of driving

white-to-opaque switching when ectopically expressed, indicating that its dosage may modulate switching thresholds in the trisomic background (Lohse et al., 2016).

A possible hypothesis is therefore that regions B and D each encode partially redundant repressive inputs, through chromatin-level silencing (*SET1*), direct transcriptional corepression (*TUP1*), and signal-responsive transcription factor activity (*RIM101*), and that only when dosage of multiple repressors across both regions is simultaneously reduced, as in the BD double deletion, is the cumulative repressive threshold breached. The diversity of functional classes represented across these two regions argues against a single mechanistic bottleneck and supports a model of distributed, combinatorial suppression. Future RNA-seq comparisons between ΔB, ΔD, and BD strains would help determine which candidates are expressed in proportion to copy number and contribute most directly to the switching phenotype.

5.5 Telomere-Mediated Truncation as a Future Strategy

Telomere-mediated chromosomal truncation is a useful complement to the CRISPR segmental deletion approach. While segmental deletions remove defined internal regions, truncation allows systematic removal of progressively increasing portions of the distal chromosome arm, starting from a defined breakpoint and extending toward the telomere. This is particularly well-suited to region D dissection because it allows a continuous scan of the region without requiring individual gRNA and repair template designs for each sub-interval.

The core principle, inserting a construct containing a mapping sequence, selectable marker, and telomere seed at a defined internal locus to create a stable truncated chromosome, has been validated in other *C. albicans* contexts and exploits the organism's efficient homologous recombination machinery and tolerance for aneuploidy (Polakova et al., 2009). Once construct assembly is complete, a series of truncations at progressively centromere-proximal positions within region D will define the minimal

interval required for switching suppression. Whole-genome sequencing combined with switching assays will map this interval at high resolution.

It is also worth noting that *WOR1*, the master activator of white–opaque switching, is located on Chr1 but falls within region C, which was not significantly affected by B+D deletion. This raises the possibility that BD deletion strains retain a full complement of *WOR1* while losing repressor dosage from regions B and D, which could in principle drive switching frequencies even higher than those seen upon full Chr1 loss, where *WOR1* copy number is also reduced. This is consistent with the recent finding that *WOR1* heterozygotes show an almost complete block in switching, underscoring how sensitive the switch is to *WOR1* gene dosage (Ganser et al., 2025). Future RNA-seq comparisons between 2×Chr1 and 3×Chr1 strains would also help clarify whether genes in regions B and D are expressed in proportion to copy number, and whether repressor dosage directly tracks with Chr1 ploidy.

6. Conclusions

Chr1 copy number regulates white–opaque switching in *C. albicans*. Trisomic strains switch at low frequencies, while loss of the extra Chr1 copy drives hyperswitching. Segmental CRISPR deletions identified regions B and D as the primary switching suppressors, single deletions of either region produced moderate switching increases, but combined deletion in strain BD19 induced hyperswitching without full Chr1 loss. No single gene knockout within these regions replicated the BD phenotype, pointing to a distributed suppression network where multiple repressors act together. Notably, *WOR1*resides in region C and is unaffected by B+D deletion; given that *WOR1* dosage is a critical determinant of switching competence (Ganser et al., 2025), this may contribute to the strength of the hyperswitching phenotype in BD strains relative to full Chr1 loss. Telomere-mediated truncation of region D is under development and will allow finer dissection of the suppressive interval once construct assembly is complete.

7. References

Anderson, J., Cundiff, L., Schnars, B., Gao, M. X., Mackenzie, I., & Soll, D. R. (1989). Hypha formation in the white-opaque transition of Candida albicans. *Infection and Immunity*, 57(2), 458–467.

Braun, B. R., & Johnson, A. D. (1997). Control of filament formation in Candida albicans by the transcriptional repressor TUP1. *Science*, 277(5322), 105–109.

Ganser, C., He, P., Frazer, C., Krysan, D. J., & Bennett, R. J. (2025). Gene dosage and protein valency impact phase separation and fungal cell fate. *PLOS Genetics*, 21(8), e1011810.

Hernday, A. D., Lohse, S. L., Bhatt, D. L., Zhu, Z., Brewer, B. J., & Johnson, A. D. (2013). Structure of the transcriptional network controlling white-opaque switching in Candida albicans. *Molecular Microbiology*, 90(1), 22–35.

Hnisz, D., Majer, O., Frohner, I. E., Komnenovic, V., & Kuchler, K. (2010). The Set3/Hos2 histone deacetylase complex attenuates cAMP/PKA signaling to regulate morphogenesis and virulence of *Candida albicans*. *PLoS Pathogens*, 6(5), e1000889.

Huang, G., Wang, H., Chou, S., Nie, X., Chen, J., & Liu, H. (2006). Bistable expression of WOR1, a master regulator of white-opaque switching in Candida albicans. *Proceedings of the National Academy of Sciences USA*, 103(34), 12813–12818.

Huang, G., Yi, S., Sahni, N., Daniels, K. J., Srikantha, T., & Soll, D. R. (2010). N-acetylglucosamine induces white-to-opaque switching, a mating prerequisite in Candida albicans. *PLoS Pathogens*, 6(3), e1000806.

Jacobsen, M. D., Duncan, A. D., Bain, J. M., Johnson, E. M., MacCallum, D. M., & Odds, F. C. (2012). Mixed Candida albicans strain populations in colonized and infected mucosal tissues. *FEMS Yeast Research*, 12(5), 570–575.

Kullberg, B. J., & Arendrup, M. C. (2015). Invasive candidiasis. *New England Journal of Medicine*, 373(15), 1445–1456.

Lohse, M. B., & Johnson, A. D. (2008). Differential phagocytosis of white versus opaque Candida albicans by Drosophila and mouse phagocytes. *PLoS ONE*, 3(1), e1473.

Lohse, M. B., & Johnson, A. D. (2009). White-opaque switching in Candida albicans. *Current Opinion in Microbiology*, 12(6), 650–654.

Lohse, M. B., Ene, I. V., Craik, V. B., Hernday, A. D., Mancera, E., Morschhäuser, J., Bennett, R. J., & Johnson, A. D. (2016). Systematic genetic screen for transcriptional regulators of the *Candida albicans* white-opaque switch. *Genetics*, 203(4), 1679–1692.

Miller, M. G., & Johnson, A. D. (2002). White-opaque switching in Candida albicans is controlled by mating-type locus homeodomain proteins and allows efficient mating. *Cell*, 110(3), 293–302.

Pappas, P. G., Lionakis, M. S., Arendrup, M. C., Ostrosky-Zeichner, L., & Kullberg, B. J. (2018). Invasive candidiasis. *Nature Reviews Disease Primers*, 4, 18026.

Polakova, S., Blume, C., Zarate, J. A., Mentel, M., Jorck-Ramberg, D., Stenderup, J., & Piskur, J. (2009). Formation of new chromosomes as a virulence mechanism in yeast Candida glabrata. *Proceedings of the National Academy of Sciences USA*, 106(8), 2688–2693.

Qasim, M. N., Valle Arevalo, A., Nobile, C. J., & Hernday, A. D. (2021). The roles of chromatin accessibility in regulating the *Candida albicans* white-opaque phenotypic switch. *Journal of Fungi*, 7(1), 37.

Raman, S. B., Nguyen, M. H., Zhang, Z., Cheng, S., Jia, H. Y., Handfield, M., & Bhatt, D. L. (2006). *Candida albicans*SET1 encodes a histone 3 lysine 4 methyltransferase that contributes to the pathogenesis of invasive candidiasis. *Molecular Microbiology*, 60(3), 697–709.

Selmecki, A. M., Dulmage, K., Cowen, L. E., Anderson, J. B., & Berman, J. (2009). Acquisition of aneuploidy provides increased fitness during the evolution of antifungal drug resistance. *PLoS Genetics*, 5(10), e1000705.

Selmecki, A., Forche, A., & Berman, J. (2006). Aneuploidy and isochromosome formation in drug-resistant Candida albicans. *Science*, 313(5785), 367–370.

Selmecki, A. M., Forche, A., & Berman, J. (2010). Genomic plasticity of the human fungal pathogen Candida albicans. *Eukaryotic Cell*, 9(7), 991–1008.

Shrivastava, M., Tiwari, A., & Bhatt, G. (2025). Mechanisms of virulence and drug resistance in Candida albicans. *Canadian Journal of Microbiology*. https://doi.org/10.1139/cjm-2025-0036

Slutsky, B., Staebell, M., Anderson, J., Risen, L., Pfaller, M., & Soll, D. R. (1987). 'White-opaque transition': A second high-frequency switching system in Candida albicans. *Journal of Bacteriology*, 169(1), 189–197.

Tsong, A. E., Miller, M. G., Raisner, R. M., & Johnson, A. D. (2003). Evolution of a combinatorial transcriptional circuit: a case study in yeasts. *Cell*, 115(4), 389–399.

Vyas, V. K., Barrasa, M. I., & Fink, G. R. (2015). A Candida albicans CRISPR system permits genetic engineering of essential genes and gene families. *Science Advances*, 1(3), e1500248.

Zordan, R. E., Galgoczy, D. J., & Johnson, A. D. (2006). Epigenetic properties of white-opaque switching in Candida albicans are based on a self-sustaining transcriptional feedback loop. *Proceedings of the National Academy of Sciences USA*, 103(34), 12807–12812.

Zordan, R. E., Miller, M. G., Galgoczy, D. J., Tuch, B. B., & Johnson, A. D. (2007). Interlocking transcriptional feedback loops control white-opaque switching in Candida albicans. *PLoS Biology*, 5(10), e256.